INFECTION AND IMMUNITY, Dec. 1998, p. 5711–5724 Vol. 66, No. 12
0019-9567/98/$04.00+0

Brucella abortus Transits through the Autophagic Pathway and Replicates in the Endoplasmic Reticulum of Nonprofessional Phagocytes

JAVIER PIZARRO-CERDÁ,[1] STÉPHANE MÉRESSE,[1] ROBERT G. PARTON,[2] GISOU VAN DER GOOT,[3] ALBERTO SOLA-LANDA,[4] IGNACIO LOPEZ-GOÑI,[4] EDGARDO MORENO,[1]† AND JEAN-PIERRE GORVEL[1]*

Centre d'Immunologie INSERM-CNRS de Marseille-Luminy, Marseille, France[1]; Centre for Microscopy and Microanalysis, University of Queensland, Brisbane, Australia[2]; Department of Biochemistry, University of Geneva, Geneva, Switzerland[3]; and Departmento de Microbiologia, Universidad de Navarra, Pamplona, Spain[4]

Received 5 June 1998/Returned for modification 17 August 1998/Accepted 1 September 1998

***Brucella abortus* is an intracellular pathogen that replicates within a membrane-bounded compartment. In this study, we have examined the intracellular pathway of the virulent *B. abortus* strain 2308 (S2308) and the attenuated strain 19 (S19) in HeLa cells. At 10 min after inoculation, both bacterial strains are transiently detected in phagosomes characterized by the presence of early endosomal markers such as the early endosomal antigen 1. At ~1 h postinoculation, bacteria are located within a compartment positive for the lysosome-associated membrane proteins (LAMPs) and the endoplasmic reticulum (ER) marker sec61β but negative for the mannose 6-phosphate receptors and cathepsin D. Interestingly, this compartment is also positive for the autophagosomal marker monodansylcadaverin, suggesting that S2308 and S19 are located in autophagic vacuoles. At 24 h after inoculation, attenuated S19 is degraded in lysosomes, while virulent S2308 multiplies within a LAMP- and cathepsin D-negative but sec61β- and protein disulfide isomerase-positive compartment. Furthermore, treatment of infected cells with the pore-forming toxin aerolysin from *Aeromonas hydrophila* causes vacuolation of the bacterial replication compartment. These results are compatible with the hypothesis that pathogenic *B. abortus* exploits the autophagic machinery of HeLa cells to establish an intracellular niche favorable for its replication within the ER.**

Recent developments in the cell biology of intracellular pathogens have started to explain the strategies that microbes use to infect and develop within their host. Among them, *Brucella* spp. are gram-negative facultative intracellular pathogens that cause brucellosis, a widely distributed zoonose affecting a broad range of mammals, ranging from dolphins and domestic animals to humans (24). *Brucella* remains endemic in many developing countries, where it causes important economic losses (77). Brucellosis in humans is a debilitating disease with diverse pathological manifestations, including fever and weakness, leading to endocarditis, arthritis, meningitis, osteoarticular complications, and neurological disorders in chronic cases (12, 37). In domestic species, including cattle, sheep, and goat, the pathology is characterized by abortion due to colonization of the placenta and fetal tissues in females and by sterility in males (65).

Members of the genus *Brucella* are closely related to plant or animal pericellular or intracellular pathogens, like *Agrobacterium*, *Rhizobium*, and *Bartonella* species (47). *Brucella abortus* is able to multiply within a membrane-bounded compartment in phagocytic (5) and non-professional phagocytic (16, 17) cells. Indirect evidence suggested that brucellae inhibit the fusion between phagosomes and lysosomes (26). Ultrastructural work has shown that multiplying bacteria are located in a ribosome-lined organelle that resembles the endoplasmic reticulum (ER) (2, 16, 17, 44). More recently, we showed that *B. abortus* distributes in autophagosome-like vacuoles (53). However, the characteristics of the compartments used by the bacteria during early phases of invasion and the molecular characteristics of *Brucella*-containing phagosomes have not been described yet.

To date, many intracellular pathogens are known to block or to alter the traffic and/or maturation of their membrane-bound compartments within host cells (25, 52, 63). Membrane traffic within the phagocytic cascade is a complex process. Early models in which phagosomes fuse with lysosomes to become a phagolysosome have been complemented by other models favoring the idea that phagosomes mature progressively before fusing with lysosomal compartments (6, 68). From a growing body of work on phagosome biogenesis, the most useful information for subsequent comparison with vacuoles containing pathogens has come from the molecular characterization of phagosomes containing inert beads or fixed particles (8, 15, 68). In phagocytic cells, plasma membrane proteins are largely removed from inert particle-containing phagosomes within the first minutes of internalization (49). The presence of the monomeric GTPase rab5 in phagosomes attests to interactions between early endosomal compartments and the phagocytic pathway (14, 43). The maturation of early phagosomes into late phagosomes is then revealed by the loss of markers from early endocytic organelles and the acquisition of markers from late endocytic organelles, such as the GTPase rab7 or the mannose 6-phosphate receptors (M6PRs) (14, 51, 56). Merg-

* Corresponding author. Mailing address: Centre d'Immunologie INSERM-CNRS de Marseille-Luminy, Case 906-13288 Marseille Cedex 9, France. Phone: (33) 4 91 26 94 66. Fax: (33) 4 91 26 94 30. E-mail: gorvel@ciml.univ-mrs.fr.

† Present address: Programa de Investigación en Enfermedades Tropicales, Escuela de Medicina Veterinaria, Universidad Nacional, Heredia, Costa Rica.

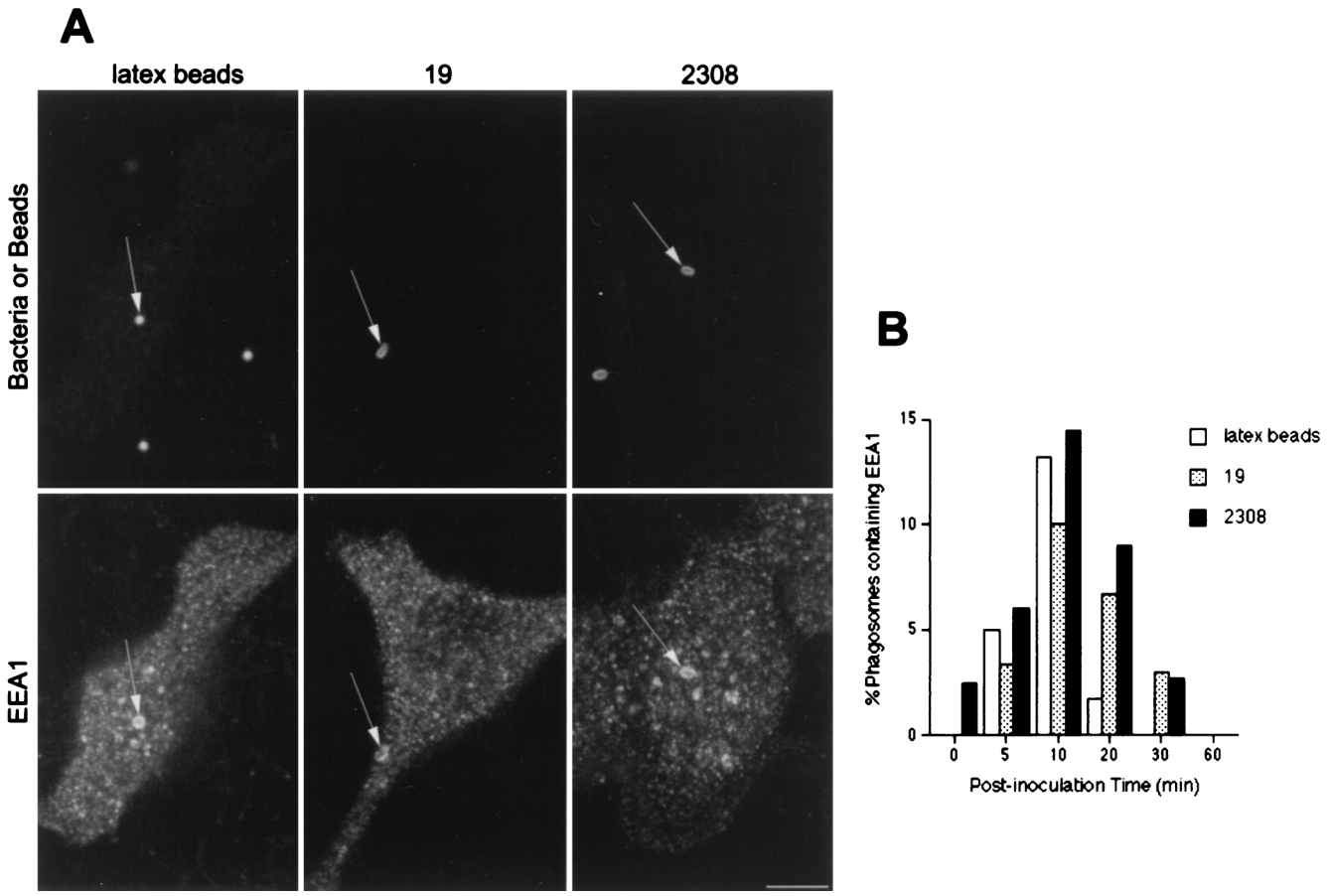

FIG. 1. EEA1 is detected in *Brucella*-containing phagosomes. HeLa cells were inoculated with S2308 or S19 or were fed with latex beads for different times up to 20 min and then were processed for single (latex beads) or double indirect immunofluorescence (for incubation times longer than 20 min, cells were washed and further incubated with fresh cell culture medium containing gentamicin). (A) Distribution of EEA1 (lower panels) and latex beads, S19, and S2308 (upper panels) at 10 min after internalization. (B) Kinetics of acquisition of EEA1 by phagosomes. Internalized particles are labeled by EEA1 (arrows in panel A), with a maximal acquisition of EEA1 at 10 min postinoculation (B). In panel B, data are averages from two different experiments. The percentage of phagosomes containing EEA1 was calculated as described in Materials and Methods. Bar, 5 μm.

ing with the lysosomal compartment is shown by the steady accumulation of lysosomal proteins such as the acid hydrolase cathepsin D or the lysosome-associated membrane proteins (LAMPs) on phagosomes (14, 49).

Intracellular pathogens are known to modify their environment in multiple ways to avoid degradation by innate host cell defense systems. In professional phagocytes, *Mycobacterium* remains within an early endosomal compartment (10, 11) that excludes the vacuolar ATPase, thus inhibiting the acidification of the bacterial phagosome (69). *Legionella pneumophila* associates to autophagosomes and takes advantage of the autophagic machinery of host cells to multiply within a ribosome-studded organelle surrounded with ER (71), rarely interacting with the endosomal cascade (61). In nonphagocytic cells, *Chlamydia trachomatis* inclusion bodies segregate completely from the endocytic pathway (31, 72) and may represent an aberrant compartment of the trans-Golgi network from where the bacterium induces the incorporation of sphingolipids into the pathogen-containing vacuole (30), which is formed mainly of proteins of chlamydial origin (58). *Coxiella burnetii* multiplies in a compartment that acidifies (55) and induces fusion of host cell lysosomes (42). *Salmonella typhimurium* bypasses late endosomal compartments and is targeted to vesicles containing lysosomal membrane glycoproteins, probably as a consequence of direct delivery from the trans-Golgi network (28). The protozoan *Toxoplasma gondii* actively invades host cells (18) and multiplies in a fusion-incompetent parasitophorous vacuole that is derived from the host plasma membrane (70) and associates with host mitochondria and ER (64). The eucaryotic unicellular flagellate *Trypanosoma cruzi* recruits lysosomes at its site of entry (73): once inside the host cell, the parasite is able to degrade the lysosomal membrane, allowing free replication in the cytosol (3). In contrast, *Shigella flexneri* and *Listeria monocytogenes* are not targeted to lysosomes but are also able to lyse their internalization compartment and replicate in the cytoplasm of infected cells (27, 32), both being capable of intracellular movement by actin-based propulsion (19, 50).

We have previously observed that *Brucella* is able to invade HeLa cells and that the virulent strain 2308 (S2308) distributes in a multimembrane, ribosome-associated compartment (53). In the present study, we detail the intracellular traffic of both virulent and attenuated *Brucella* strains in HeLa cells, and we show that both strains are able to associate with autophagosomes bypassing late but not early endosomal compartments. At later infection times, the virulent strain is delivered to the host ER, where massive intracellular bacterial replication occurs, whereas the nonpathogenic strain is degraded after fusion of its vacuole with lysosomes.

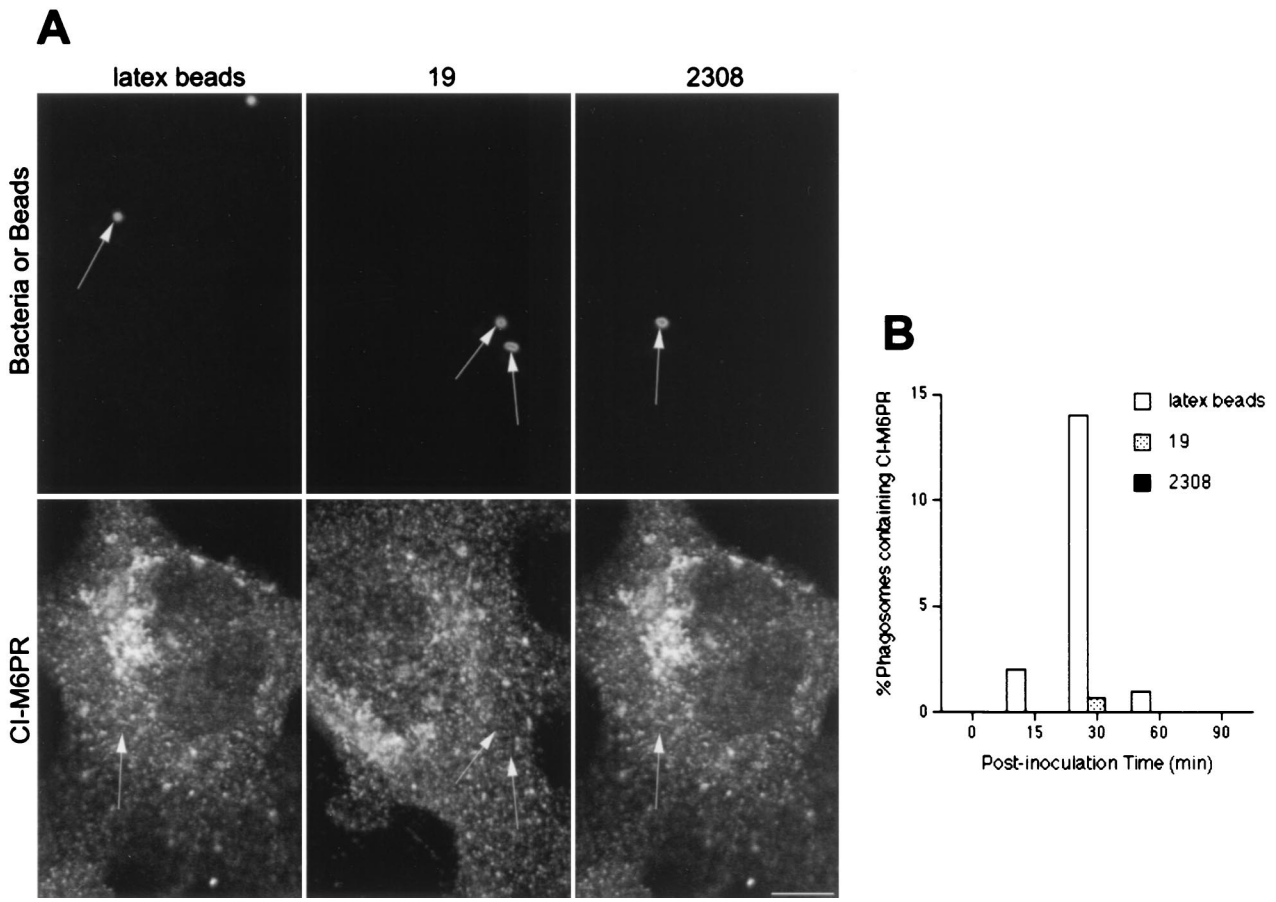

FIG. 2. *Brucella*-containing phagosomes avoid interaction with CI-M6PR-positive compartments. HeLa cells were fed with latex beads or inoculated with S2308 or S19 for different times and processed for immunofluorescence as described in the legend to Fig. 1. (A) Distribution of CI-M6PR (lower panels) and latex beads, S19, and S2308 (upper panels) at 30 min after inoculation. (B) Kinetics of acquisition of CI-M6PR by phagosomes. Note that only latex beads are decorated by anti-CI-M6PR antibodies (arrows in panel A). At 30 min postinoculation, some S19 bacteria are found in late phagosomes, while maximal acquisition of CI-M6PR is observed at 30 min in latex bead-containing phagosomes (B). In panel B, data are averages from two different experiments. The percentage of phagosomes containing CI-M6PR was calculated as described in Materials and Methods. Bar, 5 μm.

MATERIALS AND METHODS

Bacteria. *B. abortus* S19 is an attenuated smooth strain used worldwide as a live vaccine (Professional Biological Co., Denver, Colo.); S2308 is a CO_2-independent virulent smooth strain (provided by J.-M. Verger, INRA, Nouzilly, France); and S2.13, S65.21, and S65.21-*bvrR* have been described previously (66). Bacteria were grown at 37°C in tryptic soy broth (TSB) (Difco, Detroit, Mich.) to stationary phase, and aliquots were frozen at −70°C in TSB–30% glycerol. For each experiment, a log-phase culture of bacteria was prepared by incubating 50 μl of a thawed aliquot (approximately 5×10^{10} CFU/ml) in 5 ml of TSB for 15 to 17 h at 37°C with agitation to allow bacterial growth. Bacterial numbers were determined by comparing the optical density at 600 nm with a standard curve.

Antibodies and fluorescent probes. Rabbit polyclonal anti-early endosomal antigen 1 (EEA1) (provided by H. Stenmark, The Norwegian Radium Hospital, Oslo, Norway); affinity-purified rabbit polyclonal anti-cation-independent M6PR (CI-M6PR) (B. Hoflack, Institut Pasteur de Lille, Lille, France); goat polyclonal anti-cation-dependent M6PR (K. von Figura, Universität Göttingen, Göttingen, Germany); rabbit polyclonal anti-rab7 (46); rabbit polyclonal anti-human LAMP1 and LAMP2 (M. Fukuda, The Burnham Institute, La Jolla, Calif.); rabbit polyclonal anti-cathepsin D (S. Kornfeld, Washington University School of Medicine, St. Louis, Mo.); affinity-purified rabbit anti-rab6 (B. Goud, Institut Curie, Paris, France); mouse monoclonal antigiantin (H. P. Hauri, University of Basel, Basel, Switzerland); rabbit polyclonal anti-sec61β, rabbit polyclonal anti-BiP, and rabbit polyclonal antiribophorin (B. Dobberstein, Universität Heidelberg, Heidelberg, Germany); rabbit polyclonal anticalnexin (A. Helenius, Institute of Biochemistry, Zurich, Switzerland); mouse monoclonal anti-protein disulfide isomerase (PDI) (J. Stow, University of Queensland, Brisbane, Australia); and cow as well as rabbit polyclonal anti-*B. abortus* S2308 antibodies were used. Secondary antibodies used were fluorescein isothiocyanate (FITC)-conjugated donkey anti-rabbit immunoglobulin G (IgG), FITC-conjugated donkey anti-goat IgG; FITC-conjugated donkey anti-mouse IgG, and Texas red-conjugated goat anti-cow IgG (Jackson ImmunoResearch Laboratories, Immunotech, Marseille, France) and 10-nm-gold-conjugated goat anti-mouse IgG (Chemicon International, Temecula, Calif.). Fluorescent probes used were monodansylcadaverine (MDC) and dyed latex beads (diameter, 0.798 μm) (Sigma, St. Quentin-Fallavier, France).

Animal cells. HeLa cells were grown in 75-cm^2, flasks (Falcon; Becton-Dickinson, Paramus, N.J.) at 37°C in a 5% CO_2 atmosphere in Dulbecco's minimal essential medium (GIBCO-BRL, Cergy-Pontoise, France) containing 10% fetal calf serum and 2 mM glutamine without antibiotics (cell culture medium). Cells were used between passages 1 and 15 and were split 1/10 or 1/4 twice per week. For monolayer inoculations, 24-well tissue culture plates (Falcon) were seeded with 500 μl of medium, containing 10^4 or 10^5 cells, per well (for confocal microscopy analysis, cells were deposited in 24-well tissue culture plates containing 12-mm-diameter glass coverslips).

Bacterial inoculation and uptake of latex beads. We previously established a protocol of infection of HeLa cells by various strains of *B. abortus* (53, 66). Log-phase cultures of virulent smooth *Brucella abortus* S2308, attenuated smooth *B. abortus* S19 (53), and mutants of *B. abortus* S2.13, S65.21, and S65.21-*bvrR* (66) were prepared by incubating 5×10^{10} (CFU) in 5 ml of TSB for 15 h at 37°C. After HeLa cells were grown overnight, the medium was removed from the 24-well tissue plates and cells were inoculated with 500 μl of a standardized bacterial suspension (500 bacteria/cell) or a 1/20,000 dilution of a 10% solution of dyed latex beads. Culture plates were centrifuged for 10 min at $400 \times g$ at room temperature and placed in an incubator under a 5% CO_2 atmosphere at 37°C (inoculation point). After 20 min, cells were washed five times with cell culture medium to remove nonadherent bacteria or excess latex beads, and monolayers were further incubated with cell culture medium supplemented with 50 μg of gentamicin (Sigma) per ml in order to kill extracellular brucellae. In long-term experiments, this medium was replaced twice: at 1 h with fresh medium containing 25 μg of gentamicin per ml and at 24 h with medium supplemented with 5 μg of gentamicin per ml. We previously showed that at 4 h postinoculation, one to three intracellular bacteria from S2308 and S19 were detected in each infected cell (53). Under these conditions, we observed that 35 to 55% of HeLa cells were

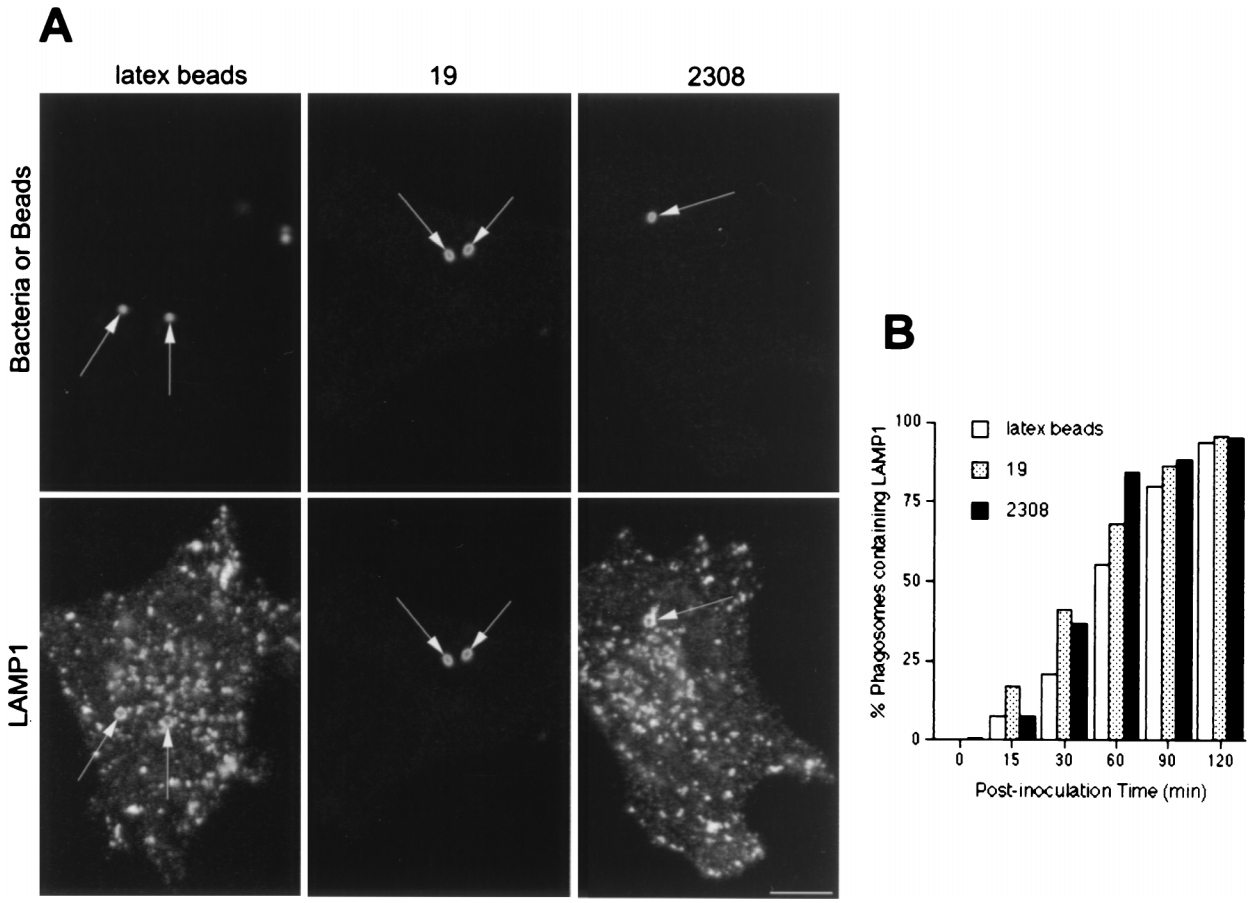

FIG. 3. LAMP1 distributes in *Brucella*-containing phagosomes. HeLa cells were fed with latex beads or inoculated with S2308 or S19 for different times and were processed for immunofluorescence as described in the legend to Fig. 1. (A) Distribution of LAMP1 (lower panels) and latex beads, S19, and S2308 (upper panels) at 1 h after inoculation. (B) Kinetics of acquisition of LAMP1 by phagosomes. LAMP1 labeling is detected in both *Brucella*- and latex bead-containing phagosomes (arrows in panel A), with >80% LAMP1-positive *Brucella*-containing phagosomes at 90 min of internalization (B). In panel B, data are averages from two different experiments. The percentage of phagosomes containing LAMP1 was calculated as described in Materials and Methods. Bar, 5 μm.

infected and that the percentage of infected cells did not vary over time (53). With the different mutants mentioned above, 100% of cells were infected with a mean of 20 extracellular bacteria and less than 1 intracellular bacterium per infected cell (66).

Analytic and quantitative immunofluorescence. At different times after inoculation, coverslips were washed to remove nonadherent bacteria (five times in cell culture medium and once in phosphate-buffered saline [PBS]) and fixed for 20 min in 3% paraformaldehyde at room temperature (or in methanol for 4 min at −20°C for detection of ER or Golgi markers). Cells were then washed once in PBS, incubated for 10 min with PBS–50% NH_4Cl in order to quench free aldehyde groups, and incubated serially with appropriate dilutions of primary antibodies directed against different host intracellular markers and with fluorescent secondary antibodies in a PBS–5% horse serum–0.1% saponin solution (30 min for each incubation, at room temperature). Monolayers were then washed in PBS and distilled water and mounted on glass slides with a Mowiol solution (Hoechst, Frankfurt, Germany). Indirect immunofluorescence and confocal analyses were performed with a TCS 4D microscope (Leica Lasertechnik Gmbh, Heidelberg, Germany) under oil immersion. To determine the percentages of bacteria or latex beads in phagosomes as characterized by the presence of the different markers used throughout the study, we first counted in the Texas red (or rhodamine) channel a minimum of 80 intracellular bacteria (revealed by indirect immunofluorescence) or latex beads (red autofluorescence emission). Intracellular bacteria or latex beads were further observed through the FITC channel to determine the percentage of particles which colocalized with the studied intracellular markers (revealed by indirect immunofluorescence).

MDC internalization. For autophagosomal labeling, cells were inoculated with bacteria for 1 h, washed five times with cell culture medium, and further incubated with serum-free cell culture medium in the presence of 50 μg of gentamicin per ml for 30 min. Monolayers were then incubated for 30 min with 500 μl of 0.05 mM MDC (7) in serum-free cell culture medium in the presence of gentamicin. Finally, cells were washed twice with cell culture medium and once with PBS and processed for indirect immunofluorescence analysis. Slides were analyzed with an MRC600 confocal microscope (Zeiss Inc., Heidelberg, Germany) equipped with the A-System filter (excitation filter, 340 to 380 nm, barrier filter, 430 nm).

Brefeldin A and proaerolysin treatment. Cells were inoculated with S2308 for 1 h and were further incubated in the presence of gentamicin (25 μg/ml) for a total period of 24 h. Infected monolayers then were treated with brefeldin A (10 μg/ml) (Sigma) for 30 min or with proaerolysin (0.38 nM) (1) for 55 min at 37°C. Monolayers were then washed, fixed, and processed for double indirect immunofluorescence analysis by using antigiantin and anti-S2308 sera for brefeldin-A-treated cells and anticalnexin and anti-S2308 sera for proaerolysin-treated cells.

Immunolabeling of frozen sections and electron microscopy. HeLa cells grown on 10-cm-diameter petri dishes were infected with bacteria for 24 h. After this inoculation period, the cells were washed with PBS and further incubated in cell culture medium supplemented with gentamicin (50 μg/ml). AT 48 h postinoculation, monolayers were washed, fixed for 1 h with a 8% paraformadehyde solution in 0.1 M phosphate buffer, and scraped from the dishes with a rubber policeman. Cells were pelleted in Eppendorf tubes, resuspended in a 10% gelatin solution, and pelleted again. The tubes were plunged in icy water to quickly solidify the gelatin and were cut open, and gelatin-embedded cell pellets were cut into small blocks and infiltrated overnight with 15% polyvinylpyrrolidone–2.3 M sucrose. The cell blocks were then mounted on the specimen stubs, immersed in liquid nitrogen, and processed for frozen sectioning in a Leica Ultracut microtome. Ultrathin sections (60 to 80 nm) for electron microscopy were transferred to Formvar-carbon-coated grids, and single immunolabeling was performed by blocking for 15 min with a PBS–2% fish skin gelatin–0.1% bovine serum albumin (BSA)–0.12% glycine solution, incubating with primary antibodies for 30 min in blocking solution, washing with a PBS–20 mM Tris–0.1% BSA solution, and incubating for 30 min with secondary antibodies in the PBS-Tris-BSA solution. Grids were treated with uranylacetate-methylcellulose and viewed with a 1010 electron microscope (Jeol, Tokyo, Japan).

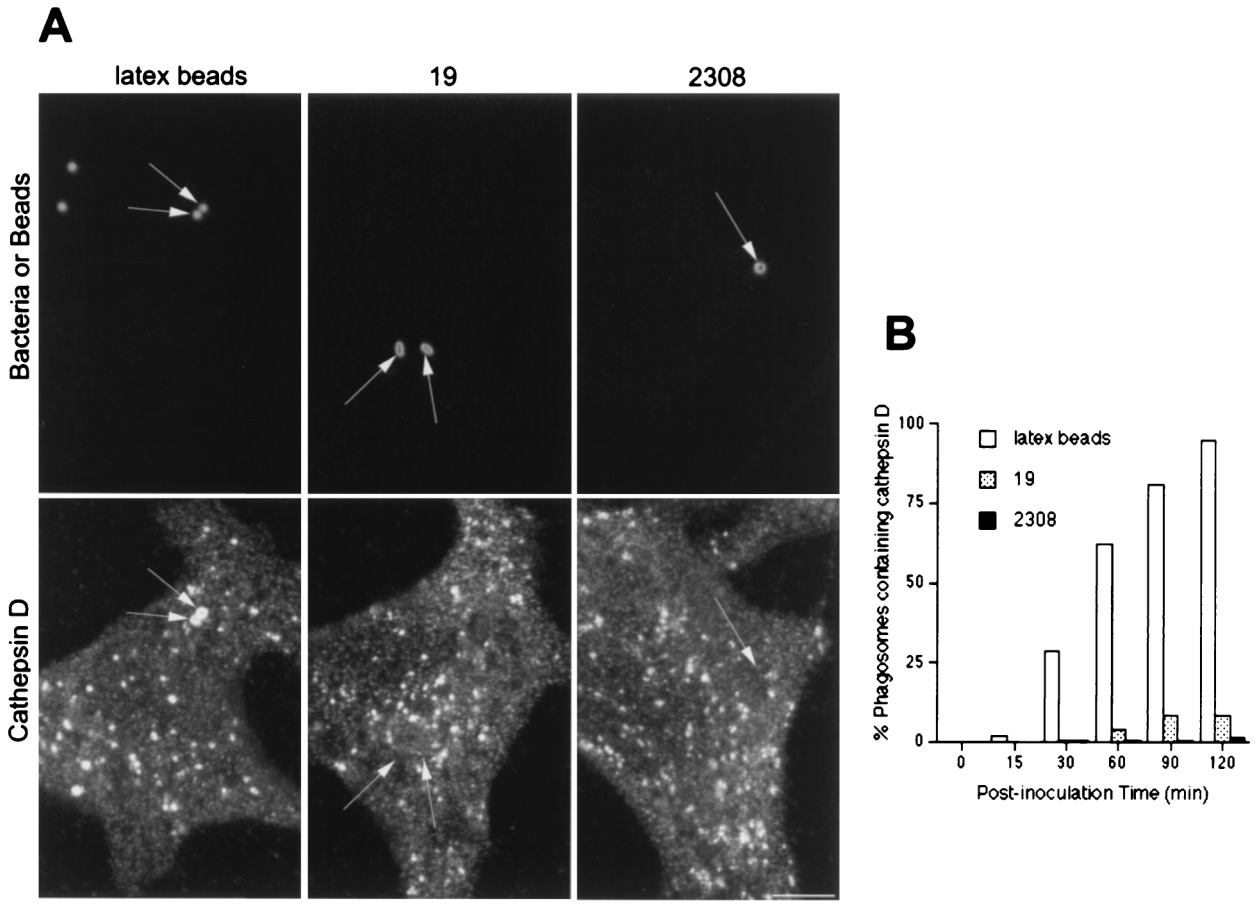

FIG. 4. Cathepsin D is not expressed in *Brucella*-containing phagosomes. HeLa cells were fed with latex beads or inoculated with S2308 or S19 for different times and processed for immunofluorescence as described in the legend to Fig. 1. (A) Distribution of cathepsin D (lower panels) and latex beads, S19, and S2308 (upper panels) at 1 h after inoculation. (B) Kinetics of acquisition of cathepsin D by phagosomes. While phagosomes containing latex beads are abundantly labeled by cathepsin D (arrows in panel A) the lysosomal marker is absent from *Brucella*-containing phagosomes (arrows in panel A). Only a few phagosomes containing S2308 (<1%) or S19 (<5%) colocalize with cathepsin D at 2 h postinoculation (B). In panel B, data are averages from two different experiments. The percentage of phagosomes containing cathepsin D was calculated as described in Materials and Methods. Bar, 5 μm.

RESULTS

Both virulent and attenuated *B. abortus* strains are first targeted to LAMP-positive, cathepsin D-negative vacuoles, bypassing late but not early endosomes. In a recent study (53), we showed that the attenuated *Brucella* strain S19 was not able to multiply efficiently within HeLa cells, unlike the virulent S2308. During S2308 infection, a lag period of ~10 h was observed, during which bacteria were found within cells but did not replicate efficiently, followed by an exponential growth period with massive bacterial replication. In the present work, we first focused on the characterization of the *Brucella*-containing phagosome during the first hours of infection and compared the intracellular fates of the virulent and attenuated strains. As a control, we internalized latex beads, which are known to transit from early to late phagosomes and merge finally into lysosomes (68).

Both S2308 and S19 were found between 5 and 15 min after inoculation in early phagosomes characterized by the presence of EEA1 (Fig. 1). The same results were observed with latex beads (Fig. 1A). These data confirm the interaction of phagosomes containing inert particles or brucellae with early endosomal compartments (43, 52). In all studied samples, between ~10 and ~15% of particles colocalized with the early endosomal markers at 10 min after inoculation (Fig. 1B). The low levels of colocalization of both bacteria and latex beads with EEA1 (~15%) suggest either their rapid and transient interaction with early endosomal compartments or that most of the bacteria or beads (~80%) avoid interactions with EEA1-positive structures. Since interactions between phagosomes containing latex beads and early endosomal compartments have been demonstrated by molecular and morphological analyses (14, 15), we favor the former hypothesis.

We next analyzed if brucellae or latex beads could be found in phagosomes expressing late endosomal markers like the prelysosomal CI-M6PR (56) or rab7 (9, 45). At 30 min after inoculation, ~20% of latex beads were found in CI-M6PR-positive compartments (Fig. 2). In contrast, S2308 was never found in CI-M6PR-positive structures (Fig. 2A), and fewer than 1% of S19 phagosomes contained the late endosomal marker (Fig. 2B). Analogous results were found when anti-rab7 or anti-CD-M6PR antibodies were used (not shown). The very low levels of prelysosomal labeling in *Brucella*-containing phagosomes compared to that of latex beads indicate that there are clear differences in the intracellular trafficking of both *Brucella* strains compared to that of inert particles.

It has been proposed that pathogenic *Brucella* strains inhibit the fusion between the bacterial compartment and lysosomes (26). Therefore, we compared the acquisitions of lysosome-associated proteins by *Brucella*- and latex bead-containing phagosomes. Both virulent and attenuated *Brucella*-containing

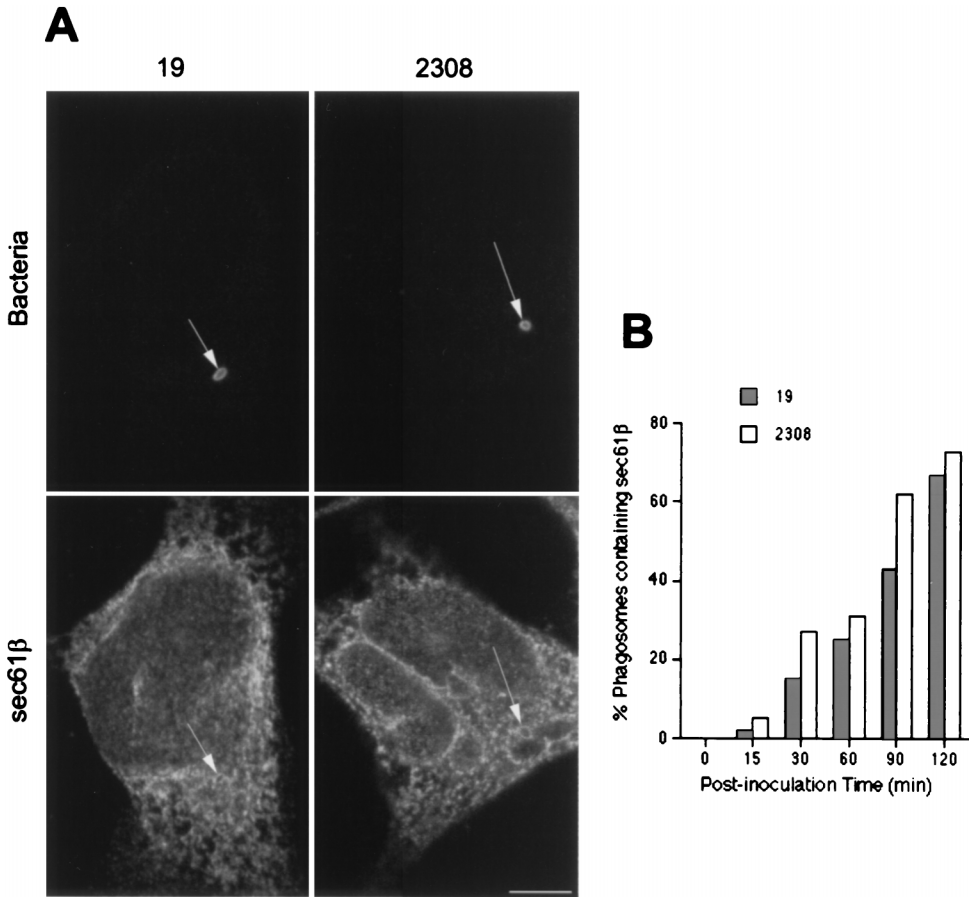

FIG. 5. *Brucella*-containing phagosomes express the ER marker sec61β. HeLa cells were inoculated with S2308 or S19 for different times and processed for immunofluorescence as described in the legend to Fig. 1. (A) Distribution of sec61β (lower panels) at 1 h postinoculation with the corresponding bacteria (upper panels). (B) Kinetics of acquisition of sec61β on phagosomes. Both S2308 and S19 are found in compartments labeled by sec61β (arrows in panel A). sec61β is incorporated in *Brucella*-containing phagosomes (B) with kinetics similar to that of LAMP1 (Fig. 3). In panel B, data are averages from two different experiments. The percentage of phagosomes containing sec61β was calculated as described in Materials and Methods. Bar, 5 μm.

phagosomes, as well as latex bead-containing phagosomes, gradually accumulated LAMP1 (Fig. 3) and LAMP2 (not shown), and at 120 min after inoculation, >95% of them were labeled for LAMP1 (Fig. 3B). In order to further characterize the possible interactions between *Brucella*-containing phagosomes and lysosomes, we analyzed the distribution of the lysosomal acid hydrolase cathepsin D. Cathepsin D was incorporated in latex bead-containing compartments with the same kinetics as LAMP1 (Fig. 3B and 4B). In contrast, at ~2 h after inoculation, this lysosomal enzyme was present in fewer than 10% of phagosomes containing virulent S2308 and in ~20% of phagosomes containing attenuated S19 (Fig. 4B). Together, these results show that while latex bead-containing phagosomes follow the phagocytic pathway from early to late compartments and finally to lysosomes, virulent and attenuated *Brucella* strains are located transiently in early phagosomes but bypass interactions with M6PR- and rab7-containing late endocytic compartments and are targeted to a LAMP1- and 2-containing compartment devoid of cathepsin D.

***Brucella* strains distribute in autophagosomes.** Using electron microscopy with Epon-embedded sections, we recently observed that *Brucella* can be found in autophagosome-like structures after infection of HeLa cells (53). Several groups have proposed that autophagosomes originate from invaginations of the ER to sequester cytoplasmic materials (23, 48). To test the possible autophagosomal origin of the LAMP-positive but cathepsin D-negative bacterial compartment, we looked for the presence of ER markers in the *Brucella*-containing phagosomes. The molecule sec61β, a subunit of the principal cross-linking partner of both type I and type II signal-anchor proteins during their membrane insertion in the ER (33), was found to decorate intracellular S2308 and S19 at ~1 h after inoculation (Fig. 5A). Latex beads were never positive for ER markers (not shown). The kinetics of sec61β incorporation in *Brucella*-containing phagosomes (Fig. 5B) were similar to those of LAMP1 (Fig. 3B). However, neither the membrane ER protein ribophorin (40) nor the luminal ER marker BiP/GRP78 (76) was found in *Brucella*-containing compartments (not shown), suggesting that bacteria may interact with a specific subcompartment originating from the ER. It has been shown that the diaminepentan autofluorescent compound MDC accumulates specifically in autophagosomes (7). This molecule was used as a probe for the detection of autophagic vacuoles in order to determine if *Brucella* distributes in MDC-positive compartments. Indeed, at 2 h postinfection both virulent S2308 (Fig. 6) and attenuated S19 (not shown) were found in compartments where the autofluorescent probe accumulated and which could be defined accordingly as autophagosomes.

Recently, Sola-Landa et al. (66) characterized the first *Brucella* two-component regulatory system described, named BvrS-BvrR for *Brucella* virulence-related sensory and regula-

tory proteins, respectively. In contrast to S2308 and S19, *bvrS* and *bvrR* mutant strains poorly invade HeLa cells and are rapidly targeted to cathepsin D-containing compartments. Therefore, we studied if these bacteria were able to transit through autophagosomes by analyzing the distribution of MDC in infected cells. As shown in Fig. 6, this marker does not label the compartments containing the mutant strain 2.13 or 65.21 (not shown), suggesting that the *bvrS bvrR* mutant brucellae are not targeted to autophagosomal compartments and demonstrating that MDC is not accumulated in a nonspecific manner in *Brucella*-containing phagosomes. S65.21-*bvrR*, harboring a plasmid construct that allows the expression of *bvrR*, recovers the virulent phenotype of S2308 (66) and access to autophagosomes labeled by MDC (not shown). We previously analyzed the intracellular distributions of both parental and mutant bacteria by double immunofluorescence in peritoneal macrophages and HeLa cells (66). In contrast to phagosomes containing the pathogenic parental *Brucella* strain, which did not fuse with cathepsin D-positive compartments, the vacuoles containing the S2.13 or S65.21 mutant were found to colocalize with cathepsin D already after 1 h of infection and degraded in lysosomes, thus following an intracellular pathway similar to that for latex beads (Fig. 3 and 4).

The S2308 replication compartment is devoid of lysosomal markers, while S19 undergoes degradation. Up to 2 h after inoculation, both virulent and attenuated *Brucella* strains seem to follow the same intracellular pathway and are located in autophagosomes. However, we previously observed that S19 is not able to multiply in HeLa cells, and at 24 h postinoculation, most of the S19 bacteria are degraded within lysosomes (53). We asked whether the autophagosome was the final compartment where intracellular bacterial replication occurs or whether the autophagic vacuole was only a transient compartment used by the virulent brucellae to reach their ultimate intracellular niche. To address this question, we studied the intracellular distributions of S19 and S2308 in infected HeLa cells during the exponential growth phase of the virulent strain, >10 h after inoculation. We first analyzed the expression of LAMPs in the *Brucella*-containing compartments. S2308-containing phagosomes excluded LAMP1 from 8 h onwards (Fig. 7B), suggesting that bacteria in the exponential phase of growth are possibly located in a compartment different from the autophagic vacuoles or induce a change in the autophagosome biochemical properties. Ultrastructural analysis of S2308-infected cells showed that rare virulent bacteria unable to exclude LAMP1 from their phagosomes presented clear signs of degradation, while healthy replicating bacteria were located in LAMP1-negative compartments (Fig. 8). In contrast, attenuated S19 and bacterial degradation products were located in LAMP1-positive vesicles (Fig. 7A). Similar results were obtained when the distribution of LAMP2 was studied (not shown). Degradation of S19 was confirmed by studying the distribution of the lysosomal marker cathepsin D in S19-containing phagosomes. S19-containing compartments gradually acquired the acid hydrolase, and at 12 h after inoculation, >95% of the S19-containing phagosomes were positive for cathepsin D (Fig. 7B), thus confirming that attenuated S19 interacted with lysosomes.

Virulent *Brucella* multiplies in the ER. Several ultrastructural studies from the group of Cheville have suggested that in Vero cells *Brucella* multiplies in the stacks of the rough ER (16, 17). To address this question, we analyzed, at 24 h postinoculation, the presence of ER markers in the bacterium-containing compartments. sec61β labeling was present in the S2308 replication compartment located at the perinuclear regions of host cells (Fig. 9). The same result was observed when we studied the distribution of the ER membrane-bound lectin

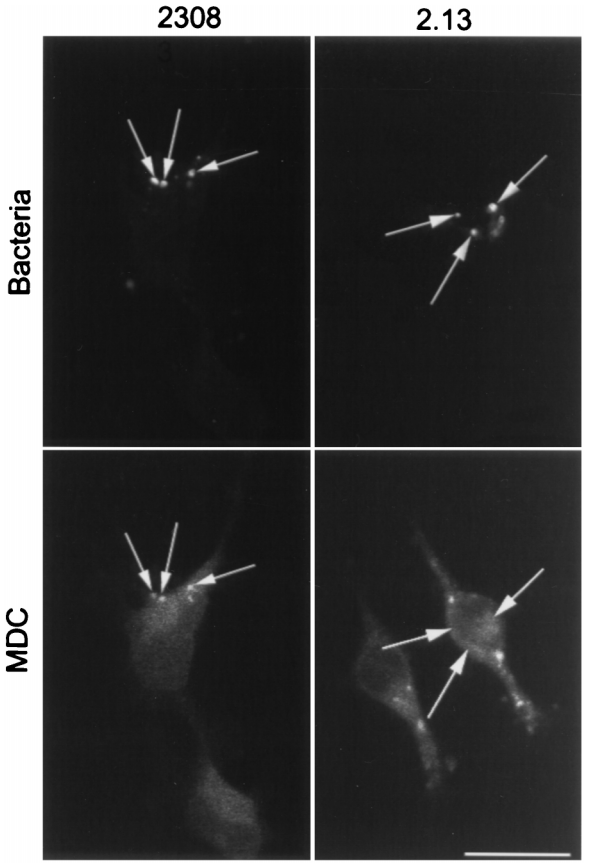

FIG. 6. MDC colocalizes with S2308-containing phagosomes. HeLa cells were inoculated for 1 h with S2308 or S2.13, washed, and further incubated for 30 min with cell culture medium depleted of fetal calf serum and glutamine and supplemented with gentamicin. Monolayers were then incubated for 30 min with MDC (0.05 mM), washed, and processed for immunofluorescence. Only vesicles containing S2308 (arrows) are abundantly labeled with MDC. Bar, 10 μm.

calnexin (74) in S2308-infected cells (Fig. 9). Interestingly, bacteria present in vesicles released from cells that exploded due to massive intracellular multiplication were positive for sec61β (not shown), suggesting that strong interactions exist between brucellae and the compartment containing this ER marker. Although there was not a clear colocalization between the brucellae and ribophorin or BiP, the ER immunofluorescence signal was more intense in the perinuclear region where bacterial replication occurred (not shown).

The intracellular niche where bacterial replication occurs could possess some ER markers but may not retain functional features of the ER or may not be recognized as ER by the host cell. In order to study this point, we next took advantage of the fungal metabolite brefeldin A, which causes a rapid redistribution of the Golgi constituents into the ER (39). We reasoned that if the *Brucella* replication compartment retains the ability to be recognized as ER, brefeldin A treatment should induce the colocalization of Golgi markers with the bacterial compartment. Cells were inoculated with S2308 for 1 h and were further incubated in the presence of gentamicin for a total period of 24 h. Infected monolayers were then treated with brefeldin A (10 μg/ml) for 30 min, washed, fixed, and processed for immunofluorescence with antiserum recognizing the Golgi marker giantin (57). As shown in Fig. 10A, after brefeldin A treatment, the Golgi compartment redistributed into ER and closely matched with the intracellular distribution of multiplying

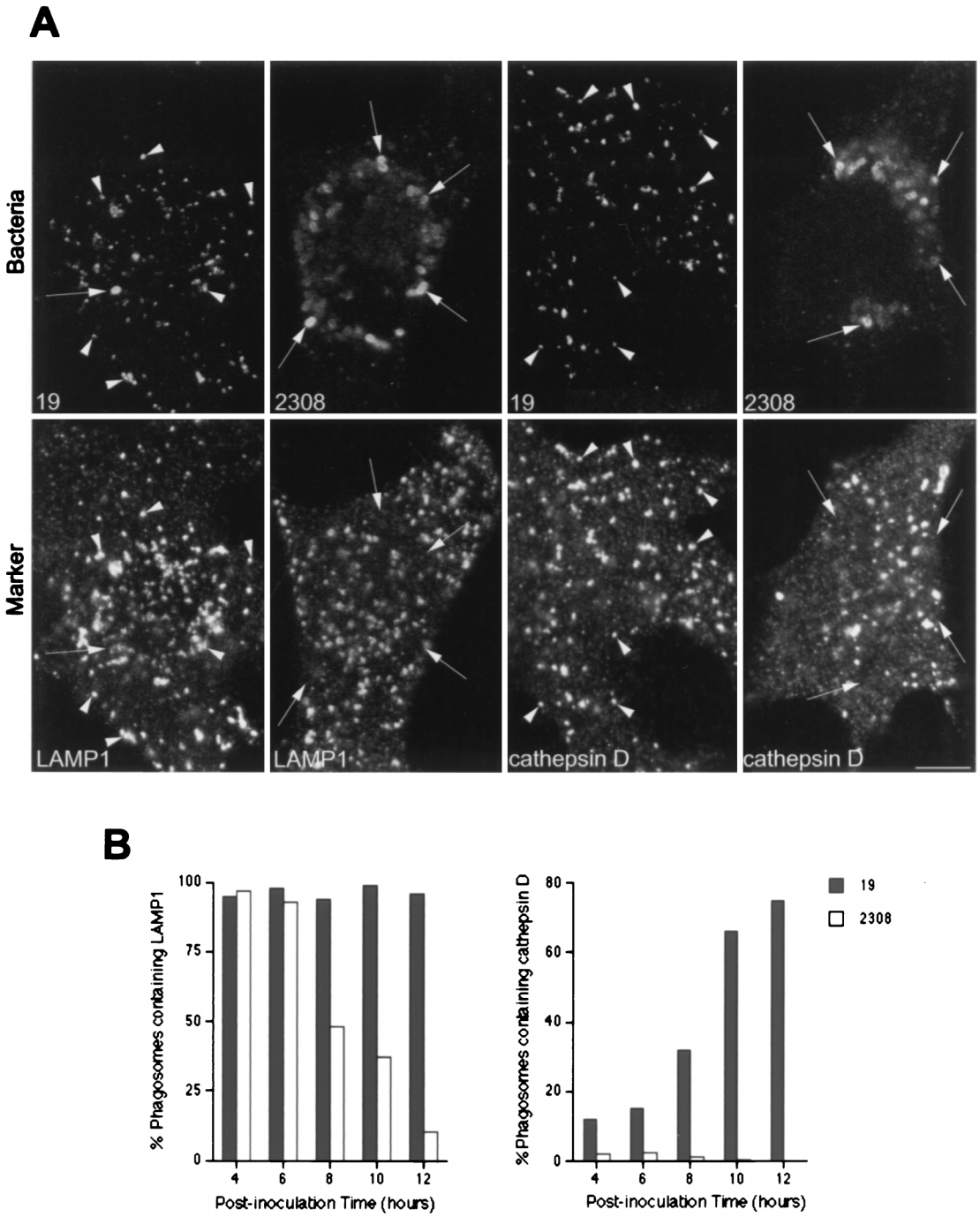

FIG. 7. S2308 multiplies in LAMP1- and cathepsin D-negative compartments. HeLa cells were inoculated for 1 h with S2308 and S19, washed, and further incubated with cell culture medium with gentamicin. At different times postinoculation, monolayers were fixed and processed for double indirect immunofluorescence. (A) Distribution of LAMP1 (two lower left panels) and cathepsin D (two lower right panels) with the indicated bacteria (upper panels) at 24 h after inoculation. (B) Kinetics of LAMP1 (left panel) and cathepsin D (right panel) acquisition in phagosomes. S19 is degraded after 24 h postinoculation (A), and both intact bacteria (arrows) and degradation products (arrowheads) colocalize with the lysosomal markers LAMP1 and cathepsin D. Moreover, S19 gradually acquires cathepsin D (B, right panel). S2308 is able to multiply in a LAMP1 and cathepsin D-negative compartment (A). LAMP is excluded from the S2308-containing phagosomes from 8 h after inoculation onwards (B, left panel). In panel B, data are averages from two different experiments. The percentages of phagosomes containing LAMP1 or cathepsin D were calculated as described in Materials and Methods. Bar, 5 μm.

S2308, suggesting that the replication compartment for *Brucella* retains at least one functional feature of the ER and can be identified as such by the infected cell. Similar results were obtained with an anti-rab6 serum (not shown).

In addition, we studied the activity of the pore-forming toxin aerolysin from *Aeromonas hydrophila* in *Brucella*-infected cells. Abrami et al. (1) have demonstrated that after binding of the protoxin to an 80-kDa glycosylphosphatidylinositol-anchored protein on BHK cells, the proaerolysin is processed to its mature form by host cell proteases and creates a channel that causes a dramatic vacuolation of the ER. HeLa cells treated with proaerolysin showed a selective disorganization of the ER

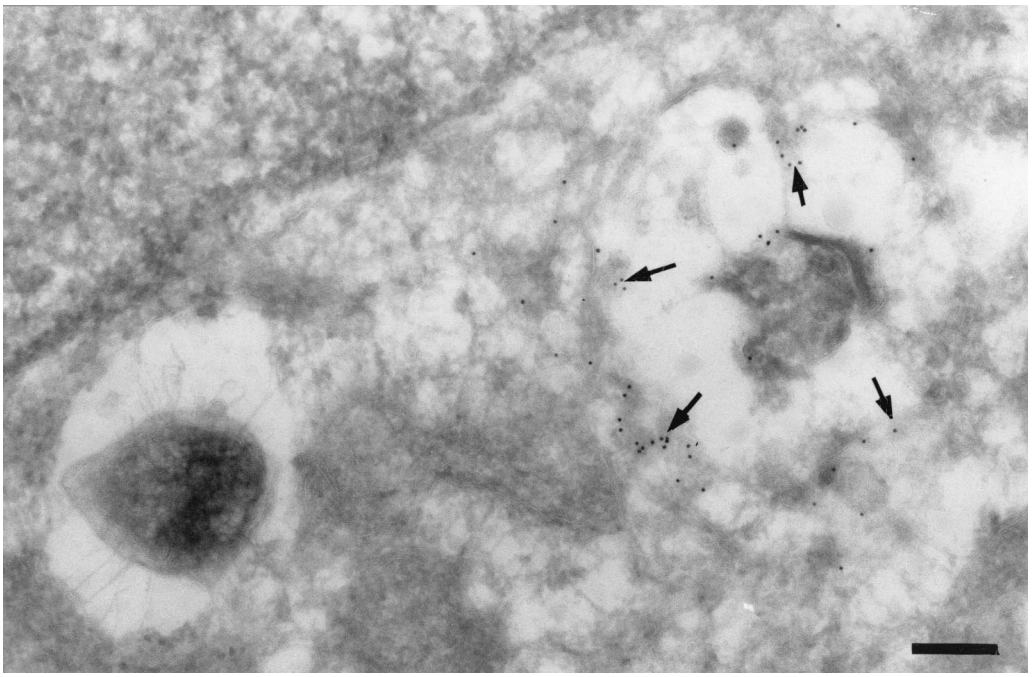

FIG. 8. Rare S2308 organisms are detected in LAMP1-positive compartments at 48 h after inoculation. HeLa cell monolayers were infected for 24 h with S2308, washed, and further incubated in cell culture medium with gentamicin for an additional 24 h. Monolayers were then fixed and processed for frozen sectioning, immunolabeling, and electron microscopy analysis. Sections were labeled for LAMP1 followed by 10-nm-gold-conjugated antibody. The micrograph shows two bacteria. The bacterium on the right shows signs of degradation, and its vacuole is positive for LAMP1 (arrows). In contrast, the healthy bacterium on the left is devoided of LAMP1. Bar, 200 nm.

(Fig. 10B). The bacterial replication compartment is also vacuolated and colocalizes with calnexin (Fig. 10B), confirming the retention of functional ER features by the S2308-containing niche.

The *Brucella* replication compartment was further characterized by immunoelectron microscopy. PDI, an abundant protein of the ER that catalyzes dithiol oxidation and disulfide bond reduction and isomerization (35), was present in the membrane of the compartment containing multiplying bacteria (Fig. 11) and in regions adjacent to brucellae. Together, these results confirm previous work indicating that virulent *Brucella* replicates in a perinuclear compartment that is related to the ER as shown by the presence of sec61β, calnexin, and PDI and that retains functional features of the ER, as shown by the redistribution of the Golgi over the *Brucella*-containing compartment after treatment with brefeldin A and also as demonstrated by the vacuolation of the bacterial replication compartment after treatment of infected cells with aerolysin.

DISCUSSION

Subversion of the phagocytic pathway by intracellular parasites is a general mechanism to establish an appropriate replication niche. In the present study, we present evidence that *B. abortus* is able to invade HeLa cells by interacting first with early endosomes; it then exploits the autophagic machinery of host cells and finally localizes into the ER, which can be defined as the bacterial multiplication compartment. A model depicting the *Brucella* intracellular pathway is shown in Fig. 12.

Earlier studies on *B. abortus* intracellular traffic focused mainly on relatively late events during infection (16, 17). In this study, we have examined the intracellular pathway followed by *Brucella* during the first minutes after invasion. We show that during the first ~10 min postinoculation, bacteria acquire early endosomal markers such as EEA1, demonstrating that *Brucella*-containing phagosomes are able to interact with early endosomes from HeLa cells (Fig. 1), as we previously observed in murine peritoneal macrophages (52). Interaction of intracellular parasites with early endosomal compartments is not a rare phenomenon. For instance, *Mycobacterium tuberculosis* and *Mycobacterium avium* phagosomes are known to interact with early endosomes in human monocyte-derived macrophages (10, 13). The *Mycobacterium bovis* phagosome retains the early endosomal GTPase rab5 but selectively excludes the late endosomal GTPase rab7, indicating that there is an arrest of the mycobacterial phagosome maturation in a stage between early and late phagosomes (75). Recent data suggest that *S. typhimurium* acquires EEA1 before being targeted to Lgp-containing vesicles (67a).

After a transient passage through early endosomes, *Brucella*, like *S. typhimurium* (28), bypasses late endosomal compartments (Fig. 2). However, in contrast to *Salmonella*, which is subsequently located in a lysosomal compartment, brucellae are targeted to compartments with the characteristics of autophagic vesicles (Fig. 6). Autophagy is a widely used pathway for the maintenance of cellular homeostasis (23). In response to a number of cellular conditions, organelles and portions of cytoplasm are sequestered in vacuoles called nascent autophagosomes. These vacuoles acquire degradative enzymes upon fusion with lysosomes, and the vacuolar content is degraded (23, 48). Based on histochemical and morphological observations, several origins for autophagic vacuoles have been proposed, including the ER, the Golgi complex, the plasma membrane, tubular lysosomes, and a specialized organelle for autophagosome formation named the phagophore (60). Although this controversy has not been completely resolved, a substantial amount of evidence suggests that autophagosomes are formed from ribosome-free regions of the rough ER (21, 22). We identified

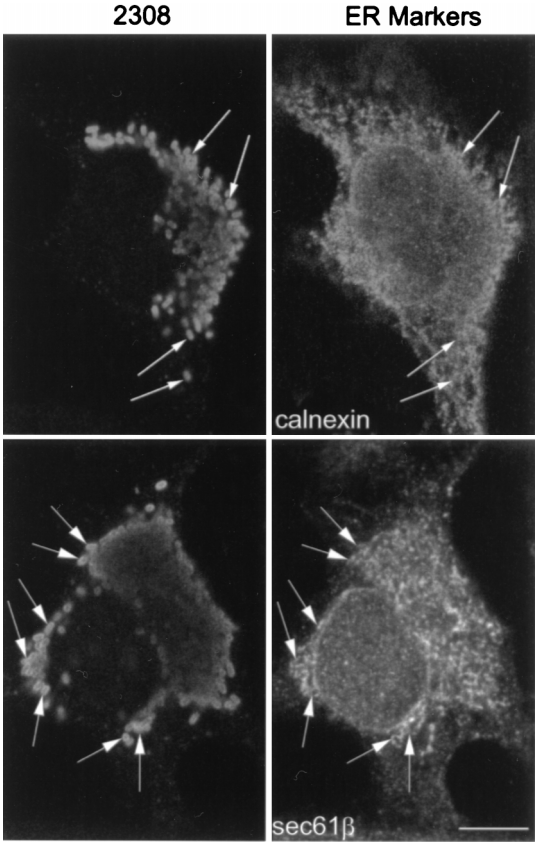

FIG. 9. S2308 multiplies in the ER. HeLa cells were infected with S2308 for 1 h, washed, and further incubated with cell culture medium supplemented with gentamicin. At 24 h after inoculation, cells were fixed and processed for double immunofluorescence. Multiplying bacteria are located in a perinuclear compartment (arrows) that matches the distribution of sec61β (lower panels) and calnexin (upper panels). Bar, 5 μm.

the *Brucella*-containing phagosomes as autophagosomes through several lines of evidence. First, the autofluorescent compound MDC, which has been shown to be specifically accumulated in autophagic vacuoles (7), colocalized with internalized bacteria at ~2 h postinoculation (Fig. 6). Second, the ER marker sec61β (but not ribophorin or BiP) was also found in *Brucella*-containing compartments (Fig. 5), together with LAMP1 and LAMP2 but not cathepsin D (Fig. 3 and 4), confirming the hypothesis of an ER-related origin for nascent autophagic vacuoles. However, Biederbick and collaborators (7) were not able to detect sec61β or the translocating chain-associating membrane protein in MDC-labeled vacuoles after subcellular fractionation of PaTu8902 cells. This suggests either that a rapid disappearance of ER-marker proteins may occur after the formation of autophagic vacuoles or that MDC accumulates only in mature autophagic vacuoles, characterized by the presence of lysosomal enzymes, such as the lysosomal acid phosphatase (7). Since we detected sec61β but not cathepsin D in *Brucella*-associated autophagosomes, this discrepancy could be explained by an accumulation of MDC in both nascent and mature autophagic vacuoles in HeLa cells. Another explanation could be that *Brucella* modifies the autophagosome properties in such a way that it allows the presence of MDC in nascent autophagic vacuoles. As stated above, the presence of other ER markers such as BiP or ribophorin in *Brucella*-containing phagosomes was not observed (Fig. 5). Work by Dunn also showed that a significant percentage of autophagosomes appear to lack rough ER proteins as determined by immunoelectron microscopy, possibly due to a recycling of proteins from autophagic vacuoles to the ER (23). Finally, we previously showed electron micrographs of *B. abortus* located in autophagic vacuoles and also demonstrated that autophagy inhibitors such as 3-methyladenine decrease bacterial yields while serum starvation increases the level of infection (41, 53).

The transit of brucellae from early endosomes to autophagosomes indicates a convergence between the autophagic and endocytic pathways. Although this question is still a matter of debate (22, 36), several groups suggest that indeed endosomes and phagosomes are able to fuse with nascent autophagic vacuoles (29, 54). Of particular interest is the work of Liou et al. (38), in which, by improving cryosectioning techniques and resolution of the different stages of autophagosome formation, it has been shown that endosomes fuse preferentially with nascent autophagosomes rather than with late autophagic vacuoles. Thus, it is conceivable that *Brucella* located in early compartments takes advantage of the convergence between endocytic and autophagic pathways to interact with nascent autophagic vacuoles. However, whether a fusion between both compartments occurs or whether early phagosomes containing *Brucella* are sequestrated by nascent autophagosomes remains to be elucidated.

The *Brucella* two-component regulatory system BvrS-BvrR has been shown to be essential for the invasion of host cells and for virulence in vivo (66). In this work we also show that *bvrS* and *bvrR* mutant strains are unable to transit through autophagic vesicles (Fig. 6), suggesting that this system is also able to sense intracellular stimuli and that access to autophagosomes is one of functions of this operon in the intracellular environment, as the complemented S65.21-*bvrR* strain recovers the capacity to enter this compartment (not shown).

Once brucellae have reached the autophagic vacuoles, the *Brucella*-containing phagosomes seem to be incompetent for fusion with endosomal compartments which have been loaded with newly exogenously administered materials. Several lines of evidence support this observation. First, bacteria that have been internalized for several hours cannot be reached by newly internalized BSA-FITC (51a). Second, intracellular *Brucella* is able to proliferate under experimental conditions in which a bactericidal concentration of gentamicin is maintained in the extracellular medium (5, 53). In contrast, in the case of a *Listeria* infection in which the bacteria are not able to escape to the cytoplasm, the antibiotic is delivered to the parasite-containing phagosome and it is killed (20).

The maturation of autophagosomes appears to occur in a stepwise manner. The first step is the acquisition of newly synthesized lysosomal membrane-associated proteins by the nascent autophagosomes. Next, acidification of the maturating compartment occurs by inclusion of the H^+-ATPase, and finally, delivery of acid hydrolases of lysosomal origin allows the degradation of intravacuolar materials (23). In fact, Aplin et al. (4) have shown that nocodazole treatment causes the accumulation of acidic autophagosomes that lack acid hydrolases, supporting the concept that vacuole acidification and acquisition of hydrolytic enzymes are separate events. The presence of LAMP1 and LAMP2 but the absence of cathepsin D at ~2 h postinoculation in S2308- and S19-containing phagosomes also supports the model of a stepwise maturation of autophagic vacuoles.

At late times (24 h) postinoculation, attenuated S19-containing phagosomes acquired cathepsin D, indicating that fusion with lysosomes had occurred (Fig. 7) and suggesting that S19 is unable to control autophagosome maturation. Consistent with these data, bacterial multiplication is minimal in S19-infected

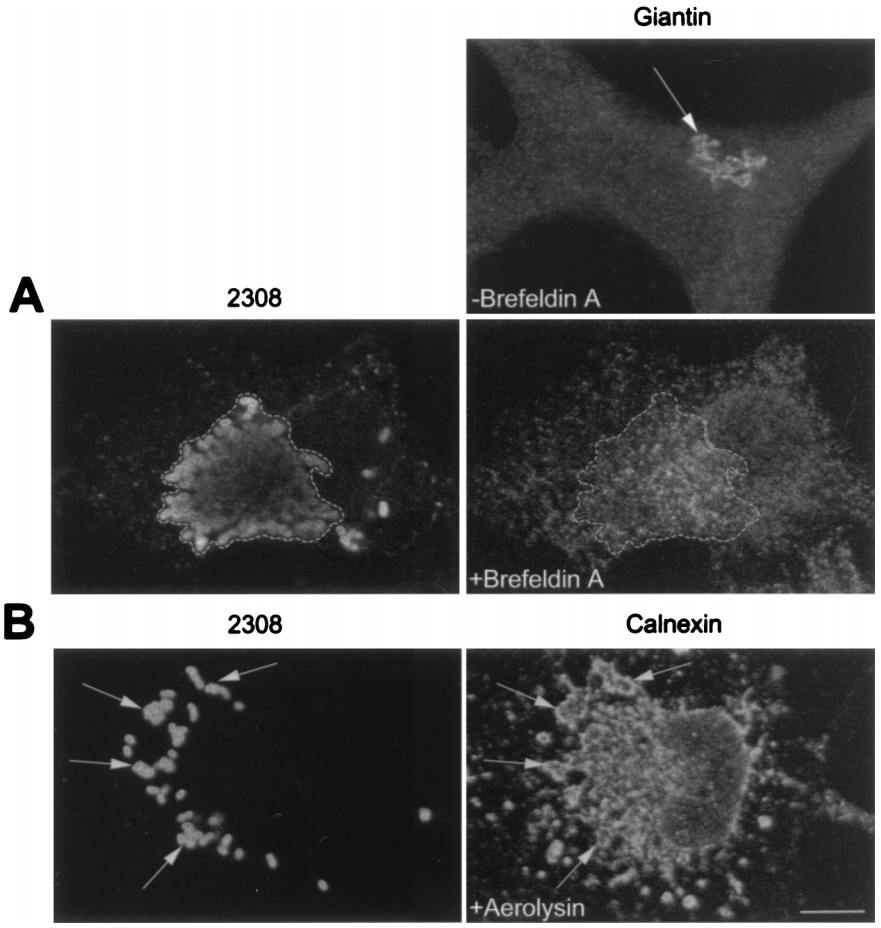

FIG. 10. The S2308 replication compartment retains functional features of the ER. Cells were infected for 1 h with S2308, washed, and further incubated with cell culture medium in the presence of gentamicin. At 24 h postinoculation, cells were incubated for 30 min with brefeldin A (10 μg/ml) (A) or for 55 min with proaerolysin (0.38 nM) (B). Monolayers were then fixed and processed for double indirect immunofluorescence. (A) The upper right panel shows the distribution of the Golgi compartment (as detected by an antigiantin antibody [arrow]) in a nontreated cell. The lower panels show the distributions of giantin (right panel) and S2308 (left panel) in the same brefeldin A-treated cell. The Golgi is redistributed in an intracellular location that matches the distribution of the bacteria (as defined by the region delimited by the dotted line). (B) Distributions of calnexin (right panel) and S2308 (left panel) in a proaerolysin-treated cell. The bacterial replication compartment is disorganized and colocalizes with the vacuolated ER (arrows). Bar, 5 μm.

cells at 48 h postinoculation (53), and bacterial degradation products are observed scattered throughout the host cell cytoplasm (Fig. 7). S19 is an avirulent strain obtained by spontaneous mutation, and its only genetic defect known to date is a deletion in the erythritol catabolic genes (59). Decreased virulence has been attributed to its inability to metabolize erythritol (67). However, it is unlikely that deficiencies in erythritol metabolism are responsible for its inability to multiply in HeLa cells. As the critical difference between S19 and S2308 seems to be the inhibition of autophagosome maturation by the latter strain, we propose that the reduced pathogenicity of S19 lies in its incapacity to respond to environmental stimuli present in the autophagosome (acidification, for example) that could activate virulence genes for the expression of important proteins for remodeling the autophagosome. In the absence of this stress response, acid hydrolases are delivered to the S19-containing autophagosome, and bacterial destruction occurs.

The autophagosome is not the replication compartment for S2308. As shown in Fig. 7, multiplying bacteria are found in a compartment that is devoid of LAMP1 and that is not labeled by MDC (not shown). In contrast, sec61β is retained from the early stages of infection and calnexin labeling is observed (Fig. 9), indicating that *Brucella*-containing phagosomes interact with the ER, as suggested by previous work (2, 16, 17, 44). The strong labeling of the *Brucella* multiplication compartment with the anti-sec61β and anticalnexin antibodies and the weak labeling with anti-BiP or antiribophorin antibodies could be interpretated as being due to interactions with a specific ER subcompartment. Another protein ubiquitously present in the ER, PDI, was detected at the membrane of the *Brucella* multiplication compartment, emphasizing the interactions of the S2308-containing compartment and the ER. The facts that brefeldin A induces the redistribution of the Golgi complex around the bacteria and that proaerolysin induces the vacuolation of the bacterial replication compartment suggest that S2308 bacteria are able to associate with a compartment that retains functional properties of the ER.

Another bacterial pathogen that is known to associate with the autophagic machinery of host cells to establish infection is *L. pneumophila* (71). There are similarities and differences between the invasion strategies of *Brucella* and *Legionella*. While *Legionella* is internalized by a process called coiling phagocytosis (34), *Brucella* seems to be internalized by zippering phagocytosis (53a). In both cases, the autophagic vacuole is associated with ribosomes. Swanson and Isberg (71) note that the presence of ribosomes on the *L. pneumophila* replication

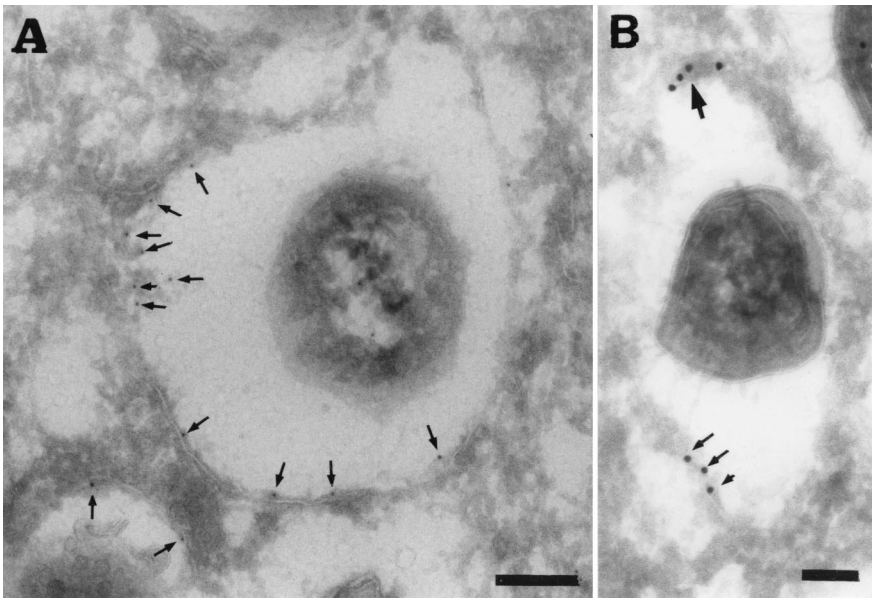

FIG. 11. S2308 is located in a PDI-positive compartment. HeLa cell monolayers were infected for 24 h with S2308, washed, and further incubated in cell culture medium with gentacimin for additional 24 h. Monolayers were then fixed and processed for frozen sectioning, immunolabeling, and electron microscopy analysis. Sections were labeled for PDI followed by 10-nm-gold-conjugated antibody. Arrows indicate the specific labeling for PDI associated with the bacterium-containing vacuoles. (A) Bar, 200 nm. (B) Bar, 100 nm.

vacuole distinguishes this organelle from autophagosomes that are thought to be generated from ribosome-free rough-ER membranes. In the case of *B. abortus*, the ribosomes associated with the *Brucella*-containing phagosomes probably appear from the sequestration of free ribosomes during the process of autophagosome formation (23, 53). Swanson and Isberg (71) suggest that *Legionella* autophagosomes originate from invagination of ER directly around the already-intracellular bacteria, and the absence of a third membrane is explained as an artifact due to mild detergent treatment. However, early events (<1 h) were not studied in their work. A hypothesis would be that, like *Brucella*, *Legionella* is first internalized in an early endosomal compartment that is able to interact with already-formed autophagosomes. The absence of the third membrane could be explained as a fusion of the endosomal compartment with the nascent autophagosomes. However, how this fusion could be achieved and how bacteria are finally found in a double-membrane-bounded compartment remain to be explained. Upon *Legionella* infection, brefeldin A treatment induces the redistribution of the Golgi complex around bacterial replication compartments, as is the case with *Brucella*.

Association of *Brucella* and *Legionella* with the host ER could be explained as a means for pathogens to obtain metabolites synthesized or translocated in the ER. Although some laboratory-adapted strains grow in minimal medium with an ammonium salt as the sole nitrogen source, the nutritional requirements for *Brucella* are complex (12). Multiple amino acids are essential for growth, and the hydrolytic activity towards large proteins is very limited. Thus, the association with the host ER could be a strategy to take advantage of the ER biosynthetic enzymes, its protein-conducting channels, or peptide translocators to increase the local supply of small peptides (62).

In the present work, we have analyzed the intracellular traffic of *Brucella* in HeLa cells from the first stages of infection to the replication compartment for the bacteria, and we have shown for the first time the presence of specific intracellular markers in the *Brucella*-containing phagosomes. Further work should define the genetic mechanisms that enable *Brucella* to take advantage of the autophagic machinery. The search for virulence factors could be the basis of novel therapeutic strategies against *Brucella* and related intracellular pathogens. Moreover, the study of this fascinating parasite should provide more insights into understanding the connections between endocytosis, exocytosis, and autophagy in animal cells.

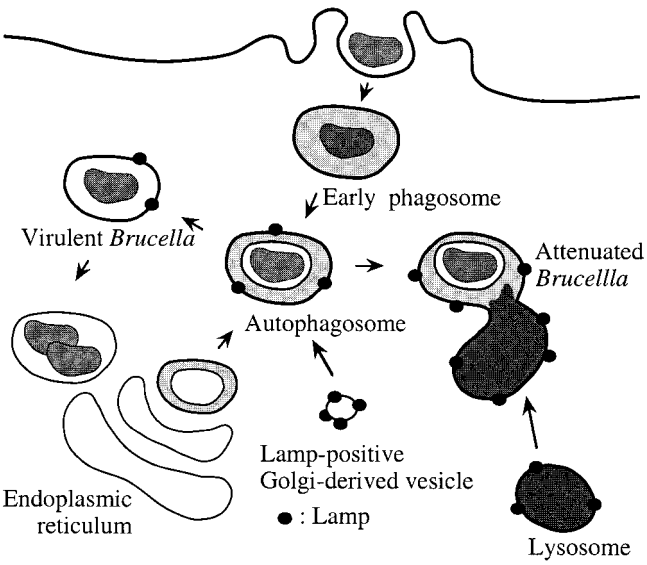

FIG. 12. Proposed model of the intracellular traffic of *B. abortus* in HeLa cells. Both virulent strain S2308 and attenuated strain S19 are found within 10 min after invasion in an early compartment positive for EEA1 that is able to fuse with autophagosomes originating from the ER and enriched by LAMP molecules possibly derived from the trans-Golgi network. S19 is then unable to inhibit the maturation of its autophagosome, which fuses with lysosomes and causes its degradation. In contrast, S2308 diverts the maturation pathway of autophagosomes and uses a retrograde transport system to access the ER, where massive replication occurs.

ACKNOWLEDGMENTS

We are grateful to Margaret Lindsay for excellent technical assistance with sample processing for frozen sectioning and electron microscopy analysis. We are indebted to Denis Allemand and Jean Jaubert for allowing us to use the confocal microscopy facilities at the Observatoire Océanologique Européen in the Centre Scientifique de Monaco.

J. Pizarro-Cerdá was supported by ICREET fellowship no. 678 from the International Union Against Cancer and is currently supported by a BDI-PVD scholarship from the Centre National de la Recherche Scientifique, France. A. Sola-Landa is supported by Fundacion Ramon Areces. This work was supported by grants from INSERM (Nord-Sud no. 4N004B and 94NS2); institutional grants from INSERM, CNRS, and LNFCC des Bouches du Rhône to J.-P. Gorvel and E. Moreno; a National Health and Medical Research Council of Australia grant (981206) to Robert G. Parton; a Swiss National Science Foundation grant to F. G. van der Goot, and a CICYT grant (BIO96-1398-C02-01) to I. Lopez-Goñi.

REFERENCES

1. **Abrami, L., M. Fivaz, P.-E. Glauser, R. G. Parton, and F. G. van der Goot.** 1998. A pore-forming toxin interacts with a GPI-anchored protein and causes vacuolation of the endoplasmic reticulum. J. Cell Biol. **140:**525–540.
2. **Anderson, T. D., and N. F. Cheville.** 1986. Ultrastructural morphometric analysis of *Brucella abortus*-infected trophoblasts in experimental placentitis. Bacterial replication occurs in rough endoplasmic reticulum. Am. J. Pathol. **124:**226–237.
3. **Andrews, N. W., and M. B. Whitlow.** 1989. Secretion by *Trypanosoma cruzi* of a hemolysin active at low pH. Mol. Biochem. Parasitol. **33:**249–256.
4. **Aplin, A., T. Jasionowski, D. L. Tuttle, S. E. Lenk, and W. A. Dunn.** 1992. Cytoskeletal elements are required for the formation and maturation of autophagic vacuoles. J. Cell. Physiol. **152:**458–466.
5. **Baldwin, C. L., and A. J. Winter.** 1994. Macrophages and *Brucella*. Immunol. Semin. **60:**363–380.
6. **Beron, W., C. Alvarez-Dominguez, L. Mayorga, and P. D. Stahl.** 1995. Membrane trafficking along the phagocytic pathway. Trends Cell Biol. **5:**100–104.
7. **Biederbick, A., H. F. Kern, and H. P. Elsässer.** 1995. Monodansylcadaverine (MDC) is a specific in vivo marker for autophagic vacuoles. Eur. J. Cell Biol. **66:**3–14.
8. **Burkhardt, J., L. A. Huber, H. Dieplinger, A. Blocker, G. Griffiths, and M. Desjardins.** 1995. Gaining insight into a complex organelle, the phagosome, using two-dimensional gel electrophoresis. Electrophoresis **16:**2249–2257.
9. **Chavrier, P., R. G. Parton, H. P. Hauri, K. Simons, and M. Zerial.** 1990. Localization of low molecular weight GTP binding proteins to exocytic and endocytic compartments. Cell **62:**317–329.
10. **Clemens, D. L.** 1996. Characterization of the *Mycobacterium tuberculosis* phagosome. Trends Microbiol. **4:**113–118.
11. **Clemens, D. L., and M. A. Horwitz.** 1995. Characterization of the *Mycobacterium tuberculosis* phagosome and evidence that phagosomal maturation is inhibited. J. Exp. Med. **181:**257–270.
12. **Corbel, M. J., and W. J. Brinley-Morgan.** 1984. Genus *Brucella* Meyer and Shaw 1920, 173^{AL}, p. 377–388. *In* N. R. Krieg and J. C. Holt (ed.), Bergey's manual of systematic bacteriology, vol. 1. The William and Wilkins Co., Baltimore, Md.
13. **de Chastelier, C., T. Lang, and L. Thilo.** 1995. Phagocytic processing of the macrophage endoparasite, *Mycobacterium avium*, in comparison to phagosomes which contain *Bacillus subtilis* or latex beads. Eur. J. Cell Biol. **68:**167–182.
14. **Desjardins, M., J. E. Celis, G. V. Meer, H. Dieplinger, A. Jahraus, G. Griffiths, and L. A. Huber.** 1994. Molecular characterization of phagosomes. J. Biol. Chem. **269:**32194–32200.
15. **Desjardins, M., L. Huber, R. Parton, and G. Griffiths.** 1994. Biogenesis of phagolysosomes proceeds through a sequential series of interactions with the endocytic apparatus. J. Cell Biol. **124:**677–688.
16. **Detilleux, P. G., B. L. Deyoe, and N. F. Cheville.** 1990. Entry and intracellular localization of *Brucella* spp. in Vero cells: fluorescence and electron microscopy. Vet. Pathol. **27:**317–328.
17. **Detilleux, P. G., B. L. Deyoe, and N. F. Cheville.** 1990. Penetration and intracellular growth of *Brucella abortus* in nonphagocytic cells in vitro. Infect. Immun. **58:**2320–2328.
18. **Doborowski, J. M., and L. D. Sibley.** 1996. *Toxoplasma* invasion of mammalian cells is powered by the actin cytoskeleton. Cell **84:**933–939.
19. **Dramsi, S., M. Lebrun, and P. Cossart.** 1996. Molecular and genetic determinants involved in invasion of mammalian cells by *Listeria monocytogenes*. Curr. Top. Microbiol. Immunol. **209:**61–77.
20. **Drevets, D. A., B. P. Canono, P. J. M. Leenen, and P. A. Campbell.** 1994. Gentamicin kills intracellular *Listeria monocytogenes*. Infect. Immun. **62:**2222–2228.
21. **Dunn, W. A.** 1990. Studies on the mechanism of autophagy: formation of the autophagic vacuole. J. Cell Biol. **110:**1923–1933.
22. **Dunn, W. A.** 1990. Studies on the mechanisms of autophagy: maturation of the autophagic vacuole. J. Cell Biol. **110:**1935–1945.
23. **Dunn, W. A.** 1994. Autophagy and related mechanisms of lysosome-mediated protein degradation. Trends Cell Biol. **4:**139–143.
24. **Enright, F. M.** 1990. The pathogenesis and pathobiology of *Brucella* infection in domestic animals, p. 301–320. *In* K. Nielsen and B. Duncan (ed.), Animal brucellosis. CRC Press Inc., Boca Raton, Fla.
25. **Finlay, B. B., and S. Falkow.** 1997. Common themes in microbial pathogenicity revisited. Microbiol. Mol. Biol. Rev. **61:**136–169.
26. **Frenchick, P. J., R. J. F. Markham, and A. H. Cochrane.** 1985. Inhibition of phagosome-lysosome fusion in macrophages by soluble extracts of virulent *Brucella abortus*. Am. J. Vet. Res. **46:**332–335.
27. **Gaillard, J. L., P. Berche, J. Mounier, S. Richard, and P. J. Sansonetti.** 1987. In vitro model of penetration and intracellular growth of *Listeria monocytogenes* in the human enterocyte-like cell line Caco-2. Infect. Immun. **55:**2822–2829.
28. **Garcia-del Portillo, F., and B. B. Finlay.** 1995. Targeting of *Salmonella typhimurium* to vesicles containing lysosomal membrane glycoproteins bypasses compartments with mannose 6-phosphate receptors. J. Cell Biol. **129:**81–97.
29. **Gordon, P. B., H. Høyvick, and P. O. Seglen.** 1992. Prelysosomal and lysosomal connections between autophagy and endocytosis. Biochem. J. **283:**361–369.
30. **Hackstadt, T., D. D. Rockey, R. A. Heizen, and M. A. Scidmore.** 1996. *Chlamydia trachomatis* interrupts an exocytic pathway to acquire endogenously synthesized sphingomyelin in transit from the Golgi apparatus to the plasma membrane. EMBO J. **15:**964–977.
31. **Heizen, R. A., M. A. Scidmore, D. D. Rockey, and T. Hackstadt.** 1996. Differential interactions with the endocytic and exocytic pathways distinguish the parasitophorous vacuoles of *Coxiella burnetii* and *Chlamydia trachomatis*. Infect. Immun. **64:**796–809.
32. **High, N., J. Mounier, M.-C. Prévost, and P. J. Sansonetti.** 1992. IpaB of *Shigella flexneri* causes entry into epithelial cells and escape from the phagocytic vacuole. EMBO J. **11:**1991–1999.
33. **High, S., S. S. Andersen, D. Gorlich, E. Hartmann, S. Prehn, T. A. Rapoport, and B. Dobberstein.** 1993. Sec61β is adjacent to nascent type I and type II signal-anchor proteins during their membrane insertion. J. Cell Biol. **121:**743–750.
34. **Horwitz, M. A.** 1984. Phagocytosis of the Legionnaires' disease bacterium (*Legionella pneumophila*) occurs by a novel mechanism: engulfment within a pseudopod coil. Cell **36:**27–33.
35. **Laboissiere, M. C., S. L. Sturley, and R. T. Raines.** 1995. The essential function of protein-disulfide isomerase is to unscramble non-native disulfide bonds. J. Biol. Chem. **270:**28006–28009.
36. **Lawrence, B. P., and W. J. Brown.** 1992. Autophagic vacuoles rapidly fuse with preexisting lysosomes in cultured hepatocytes. J. Cell Sci. **102:**515–526.
37. **Liautard, J. P.** 1996. Interactions between professional phagocytes and *Brucella* spp. Microbiologia **12:**197–206.
38. **Liou, W., H. J. Geuze, M. J. H. Geelen, and J. W. Slot.** 1997. The autophagic and endocytic pathways converge at the nascent autophagic vacuoles. J. Cell Biol. **136:**61–70.
39. **Lippencott-Schwartz, J., L. C. Yuan, J. S. Bonifacino, and R. D. Klausner.** 1989. Rapid redistribution of Golgi proteins into the ER in cells treated with brefeldin A: evidence for membrane cycling from Golgi to the ER. Cell **56:**801–813.
40. **Marcoantonio, E. E., A. Amar-Costesec, and G. Kreibick.** 1984. Segregation of the polypeptide translocation apparatus to regions of the endoplasmic reticulum containing ribophorins and ribosomes. II. Rat liver microsomal subfractions contain equimolar amounts of ribophorins and ribosomes. J. Cell Biol. **99:**2254–2259.
41. **Martys, J. L., C. Wjassow, D. M. Gangi, M. Kielian, T. E. McGraw, and J. M. Backer.** 1996. Wortmannin-sensitive trafficking pathways in Chinese hamster ovary cells. Differential effects on endocytosis and lysosomal sorting. J. Biol. Chem. **271:**10953–10962.
42. **Maurin, M., A.-M. Benoliel, P. Bongrand, and D. Raoult.** 1992. Phagolysosomes of *Coxiella burnetii*-infected cell lines maintain an acidic pH during persistent infection. Infect. Immun. **60:**5013–5016.
43. **Mayorga, L. S., B. Francisco, and P. D. Stahl.** 1991. Fusion of newly formed phagosomes with endosomes in intact cells and in a cell-free system. J. Biol. Chem. **266:**6511–6517.
44. **Meador, V. P., and B. L. Deyoe.** 1989. Intracellular localization of *Brucella abortus* in bovine placenta. Vet. Pathol. **26:**513–515.
45. **Méresse, S., J.-P. Gorvel, and P. Chavrier.** 1995. The GTPase rab7 is involved in the transport between late endosomes and lysosomes. J. Cell Sci. **108:**3349–3358.
46. **Méresse, S., P. André, Z. Mishal, M. Barad, N. Brun, M. Desjardins, and J.-P. Gorvel.** 1997. Flow cytometric sorting and biochemical characterization of the late endosomal rab7-containing compartment. Electrophoresis **14:**2682–2688.
47. **Moreno, E., E. Stackebrandt, M. Dorsch, J. Wolters, M. Busch, and H. Mayer.** 1990. *Brucella abortus* 16S rRNA and lipid A reveal a phylogenetic

relationship with members of the alpha-2 subdivision of the class *Proteobacteria.* J. Bacteriol. **172:**3569–3576.
48. **Mortimore, G. E., G. Miotto, R. Venerando, and M. Kadowaki.** 1996. Autophagy, p. 93–135. *In* M. Lloyd and J. Mason (ed.), Subcellular biochemistry, vol. 27. Biology of the lysosome. Plenum Press, New York, N.Y.
49. **Oh, Y. K., and J. A. Swanson.** 1996. Different fates of phagocytosed particles after delivery into macrophage lysosomes. J. Cell Biol. **132:**585–593.
50. **Parsot, C., and P. J. Sansonetti.** 1996. Invasion and the pathogenesis of *Shigella* infections. Curr. Top. Microbiol. Immunol. **209:**25–42.
51. **Pitt, A., L. S. Mayorga, P. D. Stahl, and A. L. Schwartz.** 1992. Alterations in the protein composition of maturing phagosomes. J. Clin. Invest. **90:**1978–1983.
51a. **Pizarro-Cerdá, J., and J.-P. Gorvel.** Unpublished results.
52. **Pizarro-Cerdá, J., E. Moreno, M. Desjardins, and J.-P. Gorvel.** 1997. When intracellular pathogens invade the frontiers of cell biology and immunology. Histol. Histopathol. **13:**1027–1038.
53. **Pizarro-Cerdá, J., E. Moreno, V. Sanguedolce, J.-L. Mége, and J.-P. Gorvel.** 1998. Virulent *Brucella abortus* avoids lysosome fusion and distributes within autophagosome-like compartments. Infect. Immun. **66:**2387–2392.
53a. **Pizarro-Cerdá, J., P. Montcourrier, and J.-P. Gorvel.** Unpublished results.
54. **Punnonen, E. L., S. Autio, H. Kaija, and H. Reunanen.** 1993. Autophagic vacuoles fuse with the prelysosomal compartment in cultured rat fibroblasts. Eur. J. Cell Biol. **6:**54–66.
55. **Rabinovitch, M., and P. S. T. Veras.** 1996. Cohabitation of *Leishmania amazonensis* and *Coxiella burnetii.* Trends Microbiol. **4:**158–161.
56. **Rabinowitz, S., H. Horstmann, S. Gordon, and G. Griffiths.** 1992. Immunocytochemical characterization of the endocytic and phagolysosomal compartments in peritoneal macrophages. J. Cell Biol. **112:**95–112.
57. **Ralston, E., and T. Ploug.** 1996. GLUT in cultured skeletal myotubules is segregated from the transferrin receptor and stored in vesicles associated with TGN. J. Cell Sci. **109:**2967–2978.
58. **Rockey, D. D., E. R. Fischer, and T. Hackstadt.** 1996. Temporal analysis of the developing *Chlamydia psittaci* inclusion by using fluorescence and electron microscopy. Infect. Immun. **64:**4269–4278.
59. **Sangari, F. J., J. M. Garcia-Lobo, and J. Aguero.** 1994. The *Brucella abortus* vaccine strain S19 carries a deletion in the erythritol catabolic genes. FEMS Microbiol. Lett. **121:**337–342.
60. **Seglen, P. O.** 1987. Regulation of autophagic protein degradation in isolated liver cells, p. 371–414. *In* H. Glaumann and F. J. Ballard (ed.), Lysosomes: their role in protein breakdown. Academic Press, Inc., New York, N.Y.
61. **Shuman, H. A., and M. A. Horwitz.** 1996. *Legionella pneumophila* invasion of mononuclear phagocytes. Curr. Top. Microbiol. Immunol. **209:**99–112.
62. **Simon, S. M., and G. Blobel.** 1991. A protein-conducting channel in the endoplasmic reticulum. Cell **65:**371–380.
63. **Sinai, A. P., and K. A. Joiner.** 1997. Safe haven: the cell biology of nonfusogenic pathogen vacuoles. Annu. Rev. Microbiol. **51:**415–462.
64. **Sinai, A. P., P. Webster, and K. A. Joiner.** 1997. Association of host cell endoplasmic reticulum and mitochondria with the *Toxoplasma gondii* parasitophorous vacuole membrane—a high affinity interaction. J. Cell Sci. **110:**2117–2128.
65. **Smith, L. D., and T. A. Ficht.** 1990. Pathogenesis of *Brucella.* Crit. Rev. Microbiol. **17:**209–230.
66. **Sola-Landa, A., J. Pizarro-Cerdá, M.-J. Grilló, E. Moreno, I. Moriyón, J.-M. Blasco, J.-P. Gorvel, and I. Lopez-Goñi.** 1998. A two-component regulatory system playing a critical role in plant pathogens and endosymbionts is present in *Brucella abortus* and controls cell invasion and virulence. Mol. Microbiol. **29:**125–138.
67. **Sperry, J. A., and D. C. Robertson.** 1975. Inhibition of growth by erythritol catabolism in *Brucella abortus.* J. Bacteriol. **124:**391–395.
67a. **Steele-Mortimer, O., and B. B. Finlay.** Unpublished results.
68. **Storrie, B., and M. Desjardins.** 1996. The biogenesis of lysosomes: is it a kiss and run, continuous fusion and fission process? Bioessays **18:**895–903.
69. **Sturgill-Koszycki, S., P. H. Schlesinger, P. Chakraborty, P. L. Haddix, H. L. Collins, A. K. Fok, R. D. Allen, S. L. Gluck, J. Heuser, and D. G. Russell.** 1994. Lack of acidification in *Mycobacterium* phagosomes produced by exclusion of the vesicular proton-ATPase. Science **263:**678–681.
70. **Suss-Toby, E., J. Zimmerberg, and G. E. Ward.** 1996. *Toxoplasma* invasion: the parasitophorous vacuole is formed from host cell plasma membrane and pinches off via a fission pore. Proc. Natl. Acad. Sci. USA **93:**8413–8418.
71. **Swanson, M. S., and R. R. Isberg.** 1995. Association of *Legionella pneumophila* with the macrophage endoplasmic reticulum. Infect. Immun. **63:**3609–3620.
72. **Taraska, T., D. M. Ward, R. S. Ajioka, P. B. Wyrick, S. R. Davis-Kaplan, C. H. Davis, and J. Kaplan.** 1996. The late chlamydial inclusion membrane is not derived from the endocytic pathway and is relatively deficient in host proteins. Infect. Immun. **64:**3713–3727.
73. **Tardieux, I., P. Webster, J. Ravesloot, W. Boron, J. A. Lunn, J. E. Heuser, and N. W. Andrews.** 1992. Lysosome recruitment and fusion are early events required for *Trypanosome* invasion of mammalian cells. Cell **71:**1117–1130.
74. **Tatu, U., and A. Helenius.** 1997. Interactions between newly synthesized glycoproteins, calnexins and a network of resident chaperones in the endoplasmic reticulum. J. Cell Biol. **136:**555–565.
75. **Via, L. E., D. Deretic, R. J. Ulmer, N. S. Hible, L. A. Huber, and V. Deretic.** 1997. Arrest of mycobacterial phagosome maturation is caused by a block in vesicle fusion between stages controlled by rab5 and rab7. J. Biol. Chem. **272:**13326–13331.
76. **Vogel, J. P., L. M. Misra, and M. D. Rose.** 1990. Loss of BiP/GRP78 function blocks translocation of secretory proteins in yeast. J. Cell Biol. **110:**1885–1895.
77. **Zavala, I., A. Nava, J. Guerra, and C. Quiros.** 1994. Brucellosis. Infect. Dis. Clin. N. Am. **8:**225–241.

Editor: P. J. Sansonetti